Homogeneous nucleation versus glass transition temperature of silicate glasses

Vladimir M. Fokin [a,1], Edgar D. Zanotto [a,*], Jürn W.P. Schmelzer [b]

[a] *Vitreous Materials Laboratory, LaMaV-DEMa, Materials Engineering Department, Federal University of São Carlos,*
P.O. Box 676, São Carlos, SP 13565-905, Brazil
[b] *Department of Physics, University of Rostock, 18051 Rostock, Germany*

Abstract

This paper provides experimental and theoretical evidence for a correlation between the maximum internal nucleation rate, $I_{max} = I(T_{max})$ [where T_{max} is the temperature of maximum nucleation rate] and the reduced glass transition temperature, T_{gr}, for 51 glass-forming liquids. In addition, it demonstrates an analogous correlation between T_{max}, the time-lag of nucleation at T_{max} and the reduced glass transition temperature. An explanation is given for these remarkable trends.
© 2003 Elsevier Science B.V. All rights reserved.

1. Introduction

Nucleation is one of the two major steps that govern the crystallization kinetics and glass-forming ability of undercooled liquids. However, nucleation rate measurements are both difficult and time consuming and cannot always be performed. Furthermore, the applicability of the classical nucleation theory (CNT) to predict nucleation rates in glasses has been a matter of widespread controversy. Hence, any correlation found between nucleation rate and structural parameters or any easily measured property of glasses is highly desirable.

Well before the development of the nucleation theory for condensed systems, Tammann called attention to the following tendency: *the higher the melt viscosity at the melting temperature, the lower its crystallizability* [1]. Qualitatively, this tendency can be explained by an increased inhibition of motion or molecular rearrangement of the basic units of the melt with increasing viscosity.

Almost eighty years after Tammann presented his ideas, James [2] and Zanotto [3,4], based on numerous experimental nucleation data for several silicate glasses, concluded that: *glasses having a reduced glass transition temperature T_{gr} ($T_{gr} = T_g/T_m$, T_g is the glass transition temperature and T_m is the melting temperature) higher than ∼0.58–0.60 display only surface (mostly heterogeneous)*

---

* Corresponding author. Tel.: +55-162 74 8250; fax: +55-162 61 5404.
E-mail address: dedz@power.ufscar.br (E.D. Zanotto).
[1] On sabbatical leave from S.I. Vavilov's State Optical Institute, 36-1 Babushkina, 193171 St. Petersburg, Russia.

crystallisation, while glasses showing volume (homogeneous) nucleation have $T_{gr} < 0.58$–0.60.

At temperatures $T < T_m$ the nucleation rate is always positive. Hence, the absence of volume nucleation data for glasses having $T_{gr} > 0.60$ only indicates undetectable nucleation on a laboratory time/size scale. Indeed, the critical cluster size and the work of critical cluster formation decreases with the difference $T_m - T$. For this reason, when the glass transition range is reached at relatively high temperatures ($T_r > 0.60$), the work of critical cluster formation is still too large to allow for measurable internal crystallization. However, close to or on interfaces, the work of critical cluster formation and the viscosity may be lower than bulk values. Therefore, surface crystallization is more commonly observed than internal crystalli-

zation. The transition from glasses demonstrating only surface crystallization ($T_{gr} > 0.60$) to glasses showing volume nucleation ($T_{gr} < 0.58$) may be qualitatively explained by an increase in nucleation rate with decreasing T_{gr}. Indeed, an increase of the magnitude of the nucleation rate with decreasing T_{gr} was demonstrated recently by Deubener [5–7] for several silicate glasses.

An additional characteristic of the nucleation process is the time-lag, which depends on both viscosity and thermodynamic driving force. Therefore, induction times and nucleation rates may be expected to follow similar general trends.

The present work provides additional experimental evidence for the above-mentioned correlation between nucleation rate and T_{gr}. The existence of an analogous correlation between the
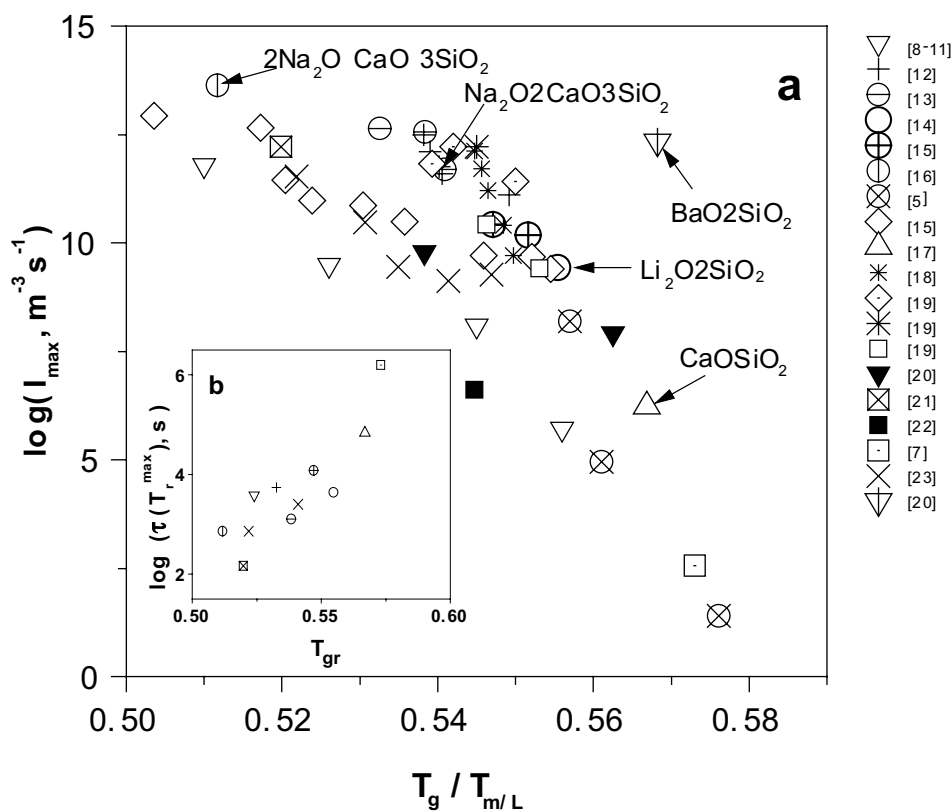

Fig. 1. (a) Maximum steady-state nucleation rate I_{max} as a function of reduced glass transition temperature, T_{gr}, for several glasses of the following systems: Na_2O–SiO_2 [8–11]; Na_2O–CaO–SiO_2 [12,16,18,19,21,22]; Na_2O–CaO–SiO_2 containing water [13,19]; Li_2O–SiO_2 [14,15,23]; Li_2O–SiO_2 containing water [15,19]; Li_2O–Na_2O–SiO_2 [5]; CaO–SiO_2 [17]; Li_2O–BaO–SiO_2 [20]; BaO–SiO_2 [20]; MgO–Al_2O_3–SiO_2 [7]. (b) Time-lag at the temperature of maximum nucleation rate as a function of T_{gr}.

Table 1
Glass compositions in mol%

N	Na_2O	CaO	Li_2O	BaO	MgO	Al_2O_3	SiO_2
1	3.3	–	30	–	–	–	66.7
2	6.6	–	26.6	–	–	–	66.7
3	10	–	23.3	–	–	–	66.7
4	34.04	15.51	–	–	–	–	50.45
5	–	–	33.5				66.5
6	–	–	33.85	–	–	–	66.15
7	–	–	34.72	–	–	–	65.28
8	–	–	36.2	–	–	–	63.8
9	–	–	37	–	–	–	63
10	–	–	37.98	–	–	–	62.02
11	–	–	38.5	–	–	–	61.5
12	–	–	39	–	–	–	61
13	–	–	41.15	–	–	–	58.85
14	–	–	–	33.3	–	–	66.7
15			34.72				65.28
16			35.12				64.88
17			36.21				63.79
18			37.09				62.91
19			38.44				61.56
20					43	14	43
21			30	3.3			66.7
22			8.3	25			67.7
23	22.5	22.5					57.5
24	39	10.7					50.3
25[a]	16.3	33.1					50.6
26[b]			33.1				66.9
27[c]			33.0				67
28		34.33					65.67
29		33					67
30	16.92	32.33					50.75
31	16.9	33.7					49.4
32	16.7	33.3					50
33	16.5	32.9					50.6
34	16	32					52
35	15.7	31.3					53
36		49.81					49.95
37[d]			33.17				66.71
38[e]			31.87				67.93
39	15	34.1					50.9
40	15.5	33.8					50.7
41	16.4	33.3					50.3
42	17	33.2					49.8
43	18.6	32.5					48.9
44			33.5				66.5
45	16.9	33.4					49.7
46[f]	16.8	33.5					49.5
47[g]	16.6	33.6					49.6
48	41						59
49	43						57
50	44						56
51	46						54

[a] 0.149 mol% H_2O. [b] 0.054 mol% H_2O. [c] 0.377 mol% H_2O. [d] 0.12 mol% H_2O. [e] 0.20 mol% H_2O. [f] 0.19 mol% H_2O. [g] 0.20 mol% H_2O.

temperature, T_{max}, of maximum nucleation rate, the induction time at T_{max}, and the reduced glass transition temperature is also demonstrated. Finally, a theoretical explanation is propounded for these important trends within the framework of the CNT.

2. Experimental nucleation rate and time-lag data

Fig. 1(a) summarizes literature data and our own values for the maximum nucleation rates, I_{max}, versus T_{gr} for 51 glasses. Glass compositions and nucleation rate parameters are presented in Tables 1 and 2. To the best of our knowledge, we have collected all the available data for silicates that present internal nucleation, extending a similar plot recently published by Deubener [5–7]. These glasses belong to eight systems: Li_2O–SiO_2, Na_2O–SiO_2, BaO–SiO_2, CaO–SiO_2, Li_2O–Na_2O–SiO_2, Na_2O–CaO–SiO_2, Li_2O–BaO–SiO_2, and MgO–Al_2O_3–SiO_2 and comprise stoichiometric (marked with arrows in Fig. 1(a)) and non-stoichiometric compositions. For non-stoichiometric compositions, the *liquidus* temperatures, T_l, were used to calculate the reduced glass transition temperature ($T_{gr} = T_g/T_l$). Fig. 1 includes data for glasses having different water contents (Li_2O–SiO_2 and Na_2O–CaO–SiO_2 systems).

The highest I_{max} ever reported for silicate glasses ($\sim 4.3 \times 10^{13}$ $m^{-3}\,s^{-1}$) refer to the nucleation of $2Na_2O$–CaO–$3SiO_2$ crystals in a glass of the same composition [16]. That is close to the upper limit of detection by optical microscopy (the technique most commonly employed in nucleation studies). The lowest I_{max} data (~ 25 $m^{-3}\,s^{-1}$), which refer to lithium disilicate crystals in a Li_2O–Na_2O–SiO_2 glass [5], are close to the lower limit determined on laboratory time/size scales. The data collected here show a clear *trend*: the higher the reduced glass transition temperature T_{gr}, the lower the I_{max}. In the relatively narrow range of T_{gr} (0.50–0.58) exhibited by these 51 glasses, the nucleation rate drops drastically by about 12 *orders* of magnitude! Hence, nucleation becomes practically undetectable at $T_{gr} \geqslant 0.58$. This finding corroborates the proposals of James [2] and Zanotto [3,4].

Fig. 1(b) shows experimental data on the time-lag, τ, for steady-state nucleation at the maximum nucleation rate temperature, T_{max}, as a function of T_{gr}. These data are not as numerous as those for nucleation rates. Nevertheless, as expected, one also finds a clear increase of the time-lag with increasing T_{gr}.

In the next section we present the theoretical background for the calculation of I_{max} and $\tau(T_{max})$ as a function of T_{gr}.

3. Theoretical background

The correlation observed between I_{max}, $\tau(T_{max})$ and T_{gr} can be qualitatively explained by the CNT. The steady-state homogeneous nucleation rate of spherical particles can be written as follows [24]:

$$I_{st} = I_0 \exp\left(- \frac{W^* + \Delta G_D}{kT} \right), \tag{1}$$

$$W^* = \frac{16\pi}{3} \frac{\sigma^3}{\Delta G_V^2}, \tag{1a}$$

where W^* is the thermodynamic barrier and ΔG_D is the kinetic barrier for nucleation, σ is the crystal/melt surface energy per unit area of crystal, ΔG_V is the thermodynamic driving force per unit volume of crystal, and I_0 is the pre-exponential term, which is slightly temperature dependent.

The temperature dependence of the nucleation rate and, consequently, the position of its maximum, T_{max}, is determined mainly by the temperature dependencies of the thermodynamic and kinetic barriers. To estimate the thermodynamic barrier, we use the crystal/melt surface energy and the thermodynamic driving force, which are given by [24]

$$\sigma = \alpha \Delta H_m V_m^{-2/3} N_A^{-1/3}, \tag{2}$$

$$\Delta G = \Delta G_V V_m = \Delta H_m \left(1 - \frac{T}{T_m} \right), \tag{3}$$

where ΔH_m is the molar heat of melting, V_m is the molar volume, N_A is Avogadro's number, and α is an empirical coefficient. These expressions bear the implicit approximations that the surface energy is size and temperature independent and the

Table 2
Glass and crystal nucleation parameters

N	Ref.	T_l (K)	T_g (K)	T_{gr}	$\log(I_{max}, \text{m}^{-3}\text{s}^{-1})$	T_{max}/T_g	$\log(\tau(T_{max}), \text{s})$
1	[6]	1273	709	0.557	8.20	1.066	
2	[6]	1237	694	0.561	4.95	1	
3	[6]	1196	689	0.576	1.40	0.933	
4	[16]	1448	741	0.512	13.64	1.050	2.86
5	[15]	1307	725	0.555	9.40		
6	[15]	1311	724	0.552	9.67		
7	[15]	1321	721	0.546	9.70		6.20
8	[15]	1339	717	0.535	10.49		
9	[15]	1348	715	0.530	10.85		
10	[15]	1360	712	0.524	10.97		
11	[15]	1366	710	0.520	11.45		
12	[15]	1372	709	0.517	12.65		
13	[15]	1397	703	0.503	12.93		
14	[20]	1693	962	0.568	12.33	1.011	
15	[23]	1322	723	0.547	9.26	1.010	
16	[23]	1330	720	0.541	9.12	1.018	3.40
17	[23]	1344	719	0.535	9.45	1.019	
18	[23]	1353	718	0.531	10.48	1.021	
19	[23]	1372	716	0.522	11.52	1.031	2.86
20	[7]	1820	1043	0.573	2.55	0.998	
21	[20]	1303	733	0.562	7.89		
22	[20]	1529	823	0.538	9.78		
23	[22]	1498	816	0.545	6.61	1.035	
24	[21]	1410	733	0.520	12.22	0.973	2.16
25	[19]	1546	844	0.545	12.22		
26	[19]	1309	724	0.553	9.42		
27	[19]	1307	714	0.546	10.42		
28	[19]	1570	851	0.542	12.22		
29	[19]	1549	852	0.550	11.42	1.043	
30	[19]	1578	851	0.539	11.82	1.034	
31	[18]	1561	850	0.545	12.11		
32	[18]	1563	853	0.546	11.71	1.019	
33	[18]	1565	855	0.546	11.20		
34	[18]	1570	861	0.548	10.41		
35	[18]	1574	865	0.550	9.70	1	
36	[17]	1817	1030	0.567	6.22	1.021	4.83
37	[15]	1307	721	0.552	10.17	0.994	
38	[15]	1307	715	0.547	10.42	0.997	4.08
39	[12]	1566	860	0.549	11.11	1.021	
40	[12]	1567	847	0.540	11.60	1.019	
41	[12]	1566	846	0.540	11.76	1.024	
42	[12]	1564	843	0.539	12.10	1.027	
43	[12]	1559	839	0.538	12.50	1.033	
44	[14]	1307	726	0.555	9.43	1.010	3.64
45	[13]	1564	846	0.541	11.70	1.043	3.74
46	[13]	1564	842	0.538	12.55	1.021	3.11
47	[13]	1564	833	0.533	12.63	1.024	3.30
48	[10]	1247	693	0.556	5.70		
49	[11]	1267	691	0.545	8.08	0.988	
50	[8]	1288	678	0.526	9.47	1.017	3.58
51	[9]	1324	675	0.510	11.77	1.086	

difference in specific heat between the crystalline and liquid phases, ΔC_p, is negligible [25]. Based on these assumptions, α is obtained from fitting nucleation experiments to the CNT and varies from about 0.40 to 0.55 for silicate glasses [26]. The replacement of Eqs. (2) and (3) for Eq. (1a) yields the following equation for the thermodynamic barrier:

$$\frac{W^*}{kT} = C_1 \frac{1}{T_r(1-T_r)^2},$$
$$C_1 \equiv \frac{16\pi}{3} \frac{\alpha^3 \Delta H_m}{RT_m}, \quad T_r \equiv \frac{T}{T_m}. \tag{4}$$

To estimate the kinetic barrier to nucleation, we use the activation energy for viscous flow, ΔG_η, thus assuming that $\Delta G_D \cong \Delta G_\eta$. ΔG_η, in turn, determines the temperature dependence of the Newtonian viscosity, η.

It is well known that silicate melt viscosity is described by the empirical equation of Vogel–Fulcher–Tammann:

$$\log(\eta) = A + \frac{B}{T - T_0}, \tag{5}$$

where A, B and T_0 are empirical constants.

This equation corresponds to a temperature dependent activation free energy $\Delta G_\eta(T)$ of the form

$$\eta = \eta_0 \exp\left(\frac{\Delta G_\eta(T)}{kT}\right), \quad \Delta G_\eta(T) = \frac{2.31kTB}{T - T_0}. \tag{6}$$

The equation for $\Delta G_\eta(T)$ can thus be rewritten as

$$\frac{\Delta G_\eta(T)}{kT} = \frac{C_2}{T_r - T_{or}}, \quad C_2 \equiv \frac{2.31B}{T_m}, \quad T_{or} \equiv \frac{T_0}{T_m}. \tag{7}$$

Experimental evidence indicates that η_0 has almost the same value for different glass-forming melts [24] ($\log \eta_0 = -4.5 \pm 1.5$); hence, parameter C_2 becomes a linear function of $(T_{gr} - T_{or})$, i.e.,

$$C_2 = C_2'(T_{gr} - T_{or}). \tag{8}$$

C_2' is determined based on the condition that, at the glass transition temperature T_{gr}, the viscosity, η, must have a well-defined value ($\sim 10^{12}$ Pa s). It follows, therefore, that C_2' is determined by

$$\ln\left(\frac{\eta(T_{gr})}{\eta_0}\right) = C_2' \tag{9}$$

with $C_2' \cong 30$ being a good approximation.

Experimental data for 14 stoichiometric oxide glasses show that T_{or} varies from 0.3 to 0.5 [30], but this variation is much smaller than that of T_{gr}, which varies from 0.3 to 0.9 [24]. Hence, for an initial approximation, we assume that T_{or} is approximately equal in all glass-forming systems. In this paper, we use $T_{or} = 0.4$. Thus, Eq. (7) has two independent parameters: C_2 and T_{or}. Hence, the viscosity and, correspondingly, T_{gr} may be varied in two different ways:

(a) C_2 can be fixed and T_{or} changed, in which case, as follows from Eq. (8),

$$T_{or} = T_{gr} - C_2/C_2' \cong T_{gr} - C_2/30. \tag{10}$$

Thus, T_{or} and T_{gr} are connected linearly, differing only by a constant.

(b) It is also possible to vary $C_2 = C_2' (T_{gr} - T_{or}) \cong 30(T_{gr} - T_{or})$ at a fixed T_{or}.

Fig. 2 shows the viscosity versus temperature plots corresponding to the above-mentioned approaches (a) and (b).

Because T_{gr} may be varied by changing either C_2 or T_{or}, the effect of T_{gr} changes on nucleation rate
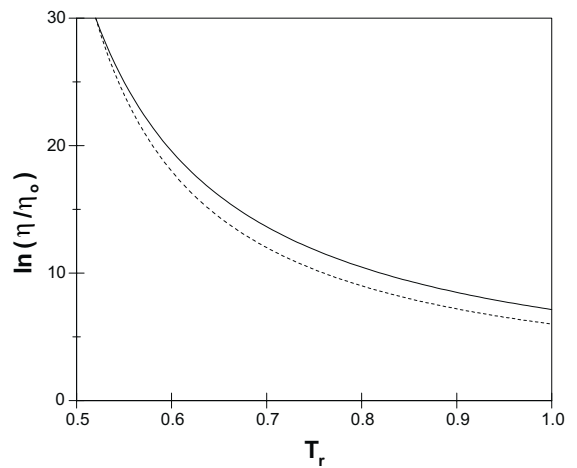

Fig. 2. Temperature dependences of $\log(\eta/\eta_0)$ corresponding to $T_{gr} = 0.52$. Solid line: $C_2 = 4.5$, T_{or} calculated from Eq. (10); dotted line: $T_{or} = 0.4$, C_2 calculated from Eq. (8).

and the time-lags may also vary. However, as shown below, in the most interesting range of temperatures, different ways of varying T_{gr} lead to surprisingly similar results. Therefore, T_{gr} can be treated as the decisive quantity for an understanding of the general trends of nucleation rate and time-lag temperature dependencies.

To calculate $I(T_r)$, we use Eq. (1) with the pre-exponential term $I_0 = 10^{42}$ m^{-3} s^{-1} and the following values of C_1 and C_2 for thermodynamic and kinetic barriers, respectively:

(i) $4.5 < C_1 < 7$, corresponding to dimensionless melting entropy $(\Delta S_m/R)$ varying from 1.6 to 6.5, if $\alpha = 0.40$–0.55 is used in Eq. (2). C_1 is related to the structural difference between the crystal and its corresponding liquid phase.
(ii) $C_2 = 4.5$ and 9.5, corresponding to 'short' and 'long' glasses, respectively. The latter parameter measures the temperature dependence of the molecules' diffusion rates in the liquid.

To estimate the time-lag for nucleation, $\tau(T_r^{max})$ versus T_{gr}, we applied the following equation [24]:

$$\tau = \frac{16}{\pi^2} \frac{h\sigma}{\Delta G_V^2 a^4} \exp\left(\frac{\Delta G_D}{kT}\right), \tag{11}$$

where h is Planck's constant and a is a quantity of the order of the 'structural units' size.

By replacing Eqs. (2) and (3) in Eq. (11) and assuming that $\Delta G_D \approx \Delta G_\eta$, Eq. (11) can be rewritten as

$$\tau = \frac{16hN_A}{\pi^2} \frac{\alpha}{\Delta H_m(1 - T_r)^2} \exp\left(\frac{\Delta G_\eta}{kT}\right). \tag{12}$$

The following values of ΔH_m and α (average for silicate glasses) were used in the calculations: $\Delta H_m = 47\,300$ J/mol; $\alpha = 0.45$. These values correspond to $C_1 = 5$ and 6 for $\Delta S_m/R = 3.3$ and 3.9, respectively.

4. Nucleation rate calculations: Results for different glass transition temperatures

The steady-state nucleation rate and the time-lag can be calculated based on the equations out-

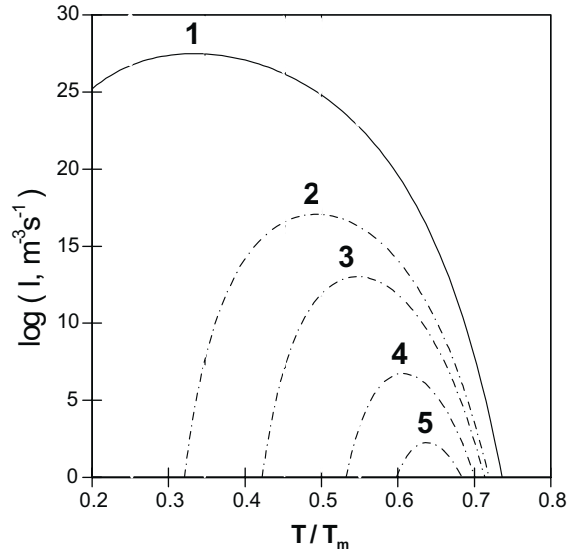lined above. Results of numerical computations are presented in Figs. 3–7.

Fig. 3. Temperature dependence of the nucleation rate calculated from CNT at fixed parameters $C_1 = 5$, $C_2 = 4.5$ (see text) for different kinetic barriers. 1 – absence of kinetic barrier; 2–5 – kinetic barriers corresponding to the different reduced glass transition temperatures T_{gr}: 0.40 (2), 0.50 (3), 0.60 (4), 0.65 (5).
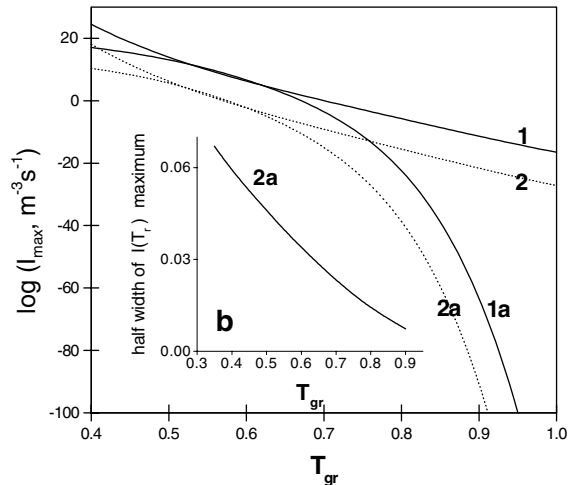

Fig. 4. Maximum nucleation rate (a) and half-width of nucleation rate curve (b) as a function of the reduced glass transition temperature. The lines are calculated from CNT with $T_{or} = 0.4$ (1, 2) and $C_2 = 4.5$ (1a, 2a) for different thermodynamic barriers (see text): $C_1 = 5$ (1, 1a), 7 (2, 2a).
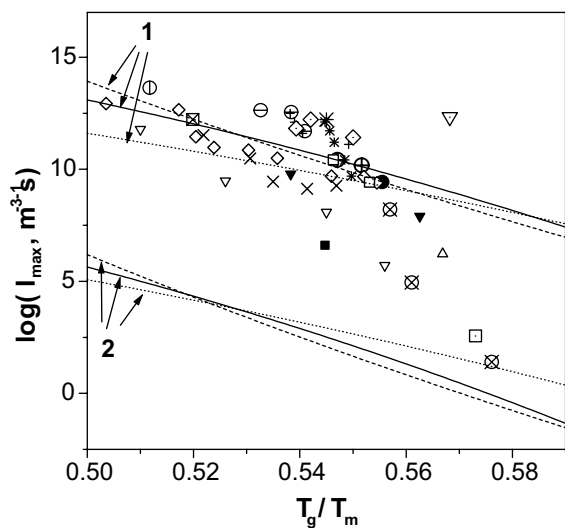
Fig. 5. Maximum nucleation rate I_{max} as a function of reduced glass transition temperature. The lines are calculated from CNT with for different thermodynamic and kinetic barriers (see text): $C_1 = 4.5$ (1), 6.5 (2); $C_2 = 4.5$ – solid lines, $C_2 = 9.5$ – dotted lines; $T_{or} = 0.4$ – dashed lines. The points are the experimental data specified as in Fig. 1.

Fig. 7. Time lag of nucleation as a function of reduced glass transition temperature. The lines are calculated from CNT with fixed C_2 (1, 2, 3, 4) and $T_{or} = 0.4$ (5, 6) for different thermodynamic and kinetic barriers: $C_1 = 4.5(1, 2, 5)$, $6.5(3, 4, 6)$; $C_2 = 4.5$ – solid lines, $C_2 = 9.5$ – dotted lines. The points refer to experimental data denoted as in Fig. 1.
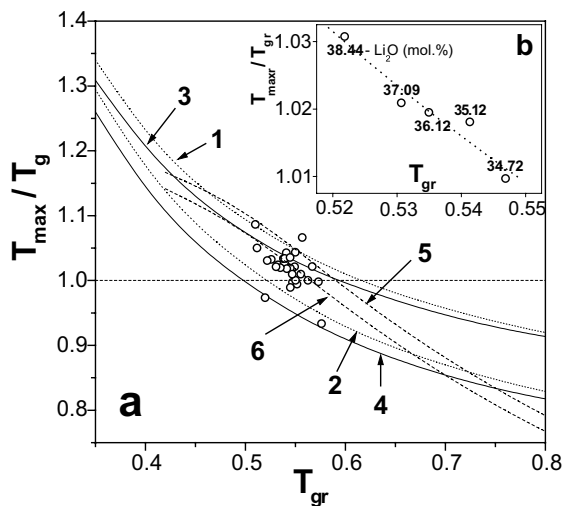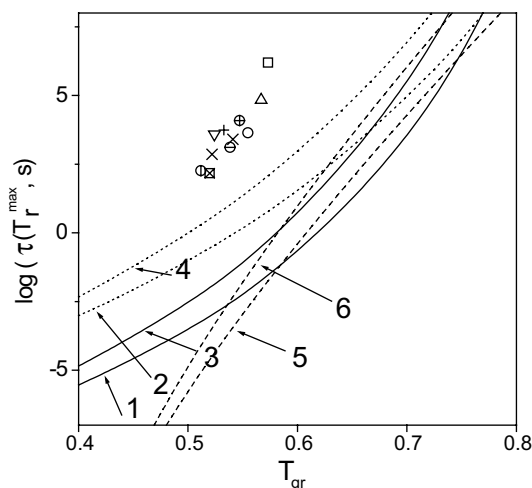

Fig. 6. (a) Ratio between the temperature of the nucleation rate maximum and the glass transition temperature as a function of the reduced glass transition temperature. The lines are calculated from CNT with two viscosity approximations (see text) for different thermodynamic and kinetic barriers: C_2 fixed, T_{or} varied – $C_1 = 4.5$ (1, 2), 6.5 (3, 4); $C_2 = 4.5$ (1, 3), $C_2 = 9.5$ (2, 4); $T_{or} = 0.4$, $C_1 = 4.5(5)$, 6.5(6). The points refer to experimental data. (b) Experimental data for Li_2O–SiO_2 glasses [23]. The numbers denote the Li_2O content in mol% by analysis. The line is placed to guide the eye.

Fig. 3 shows some typical examples of the nucleation rate temperature dependencies calculated for different reduced glass transition temperatures and, correspondingly, for different kinetic barriers.

The maximum nucleation rate temperature, T_r^{max}, the nucleation rate at T_r^{max}, $I_{max} = I(T_r^{max})$, and the half-width (h-w) of nucleation rate curve, taken from curves similar to those presented in Fig. 3, are given in Figs. 6, 4(a) and (b), respectively, as functions of the reduced glass transition temperature. The T_{max}/T_g ratio plotted in Fig. 6 as a function of T_{gr} allows one to easily estimate whether $T_{max} > T_g$ or $T_{max} < T_g$. Fig. 5 depicts an enlarged $I_{max}(T_{gr})$ plot for T_{gr} varying from 0.50 to 0.59, i.e., in the T_{gr} interval within which most of the experimental data are located. Fig. 7 illustrates the calculated induction time at T_r^{max}.

Appendix A presents a derivation of analytical expressions for I_{max} and $\tau(T_r^{max})$ as functions of the reduced glass transition temperature, demonstrating that the properties of the respective curves found numerically are valid regardless of the particular choice of parameters used in the numerical calculations.

5. Discussion

According to the CNT (see Appendix A, Eq. (A.1)), a decrease in temperature produces two effects: it not only decreases the thermodynamic barrier to nucleation (leading to a higher nucleation rate) but also increases the kinetic inhibition of nucleation due to an increase of viscosity (resulting in a lower nucleation rate). As a result of these two contrary tendencies, one finds a maximum of the steady-state nucleation rate well below T_m. For instance, as evidenced by the theory (cf. Appendix A, Eq. (A.3)), $T_r = 1/3$ is a lower limit to T_r^{max} (when the Turnbull equation is used to estimate the thermodynamic driving force (Eq. (3))). However, the kinetic inhibition of nucleation in glass-forming silicate melts is rather high. This property shifts T_r^{max} to higher temperatures in comparison to 1/3. Due to the increase of the thermodynamic barrier to nucleation with increasing temperature, this shift is accompanied by a drastic drop in the magnitude of $I(T_{max})$ [27]. These facts are illustrated in Figs. 3 and 4(a).

As shown in Fig. 4(a), $I(T_{max})$ decreases with an increase of T_{gr}, in line with expectations. If T_{gr} increases, the kinetic inhibition of nucleation proceeds at higher values of temperature and, thus, at higher values of the thermodynamic barrier. These general trends are independent of how the parameter T_{gr} is changed. Quantitatively, the results obtained by two different methods of varying T_{gr} (Fig. 4(a), curves 1, 2 and 1a, 2a) show significant differences, which are, however, most pronounced for $T_{gr} > 0.7$–0.8. In the range of practical interest ($0.5 < T_{gr} < 0.6$), the differences are very slight. The increase in T_{gr} also results in a narrowing of the half-width of the nucleation curve (Fig. 4(b)). The latter effect, together with a decreased nucleation rate, hinders the observation of homogeneous nucleation in glasses with high T_{gr}.

The results of $I_{max}(T_{gr})$ calculations are given in Fig. 5 within a narrow interval of T_{gr} (0.50–0.59). Recall that C_1 and C_2 characterise the *temperature independent* parts of the thermodynamic and kinetic barriers to nucleation (see Eqs. (4) and (7)). It should be stressed that C_1 is independent of temperature only if one assumes that the surface energy (or α) is temperature independent. On the

other hand, temperature dependent surface energy fitted to nucleation rate data is always lower than the independent one fitted from the same data. The use of temperature dependent surface energies in the present calculations results in an increase of the calculated nucleation rate maxima (increase in I_{max} and T_r^{max}) for any given T_{gr}, but the overall dependence of I_{max} and T_r^{max} on T_{gr} is not significantly changed.

In a short interval of T_{gr} (0.50–0.59), there are experimental data on homogeneous nucleation for several glasses in temperature ranges that include T_{max}. These experimental points are bounded by $\log(I_{max})$ vs. T_{gr} lines that were calculated using reasonable values of C_1 and C_2 and different ways to vary T_{gr}.

Most of the experimental data presented here refer to non-stoichiometric glasses; therefore, the change in ΔG_D caused by the deviation of the crystal composition from the melt composition should, in general, be taken into account. Moreover, we have used the Turnbull approximation for the thermodynamic driving force, but it is known that experimental ΔG are bounded by the expressions of Turnbull (upper bound) and Hoffman (lower bound) [25].

In addition, nucleation of metastable phases is possible in both stoichiometric and non-stoichiometric glasses and, thus, the ΔG used here may be inappropriate for some of these systems. BaO–$2SiO_2$, for instance, is a clear case of metastable phase formation [28]. It is relevant, within this context, to note that the data point relating to BaO–$2SiO_2$ is very dissimilar from the others! In general, thermodynamic barriers, Eq. (4), vary substantially for different glasses; thus, one has to analyse the observed trend within reasonable limits.

Nevertheless, taking into account the preceding arguments, the scattering of experimental points is acceptable. This fact presumably derives from the dominant role of the kinetic barrier at high undercoolings. It is most relevant to this paper's objectives that both experimental data and calculated curves show a clear *decrease* of I_{max} with T_{gr}. However, it should be noted that, starting at $T_{gr} \sim 0.55$, a pronounced increase in the slope is observed in the experimental data. As shown in

Fig. 6 and demonstrated analytically in Appendix A, the temperature of the nucleation rate maximum, T_r^{max}, increases with increasing T_{gr}. However, its increase is slower than that of T_{gr} and, at $T_{gr} \sim 0.55$, T_r^{max} approaches T_{gr}. Hence, beginning at $T_{gr} \sim 0.55$, $\eta(T_r^{max}) \geqslant 10^{12}$ Pa s. It is possible that, at these high viscosities, elastic stresses (neglected in this paper) may exert an influence on nucleation, providing a reason for this additional decrease in the nucleation rate, $I(T_r^{max})$, in glasses with $T_{gr} > 0.55$.

Thus, based on the above approximations, although the CNT does *not* explain perfectly the I_{max} vs. T_{gr} dependence, it does give a correct trend.

The position of the nucleation rate maximum is a significant parameter. In the case of homogeneous nucleation, it is commonly accepted that T_{max} is just *at or a little above* T_g. The calculations of $I(T)$ made for different T_{gr} clarify this statement.

According to Fig. 6, the difference between T_{max} and T_g depends on T_{gr} (see also Appendix A, Eq. (A.4)). For any combination of C_1 and C_2 and an approximation for the viscosity, there is a T_{gr} above which $T_{max} < T_g$ and below which $T_{max} > T_g$. ($T_{max} < T_g$ corresponding to points below 1 and $T_{max} > T_g$ above 1). If the Turnbull approximation is used to estimate ΔG, as T_{gr} tends to zero (liquids with very low viscosity), the maximum of $\exp(-(W^* + \Delta G_D)/kT)$ shifts to $T_{max} = T_m/3$. Therefore, $(T_r^{max} - T_{gr})$ tends to 1/3.

The points in Fig. 6 refer to experimental data for glasses that undergo homogeneous volume nucleation. Indeed, most of them correspond to $T_{max} > T_g$. However, a few points correspond to $T_{max} < T_g$. Generally speaking, there is a slight tendency for T_{max}/T_g to decrease with increasing T_{gr}. This tendency is more clearly visible if data for the same system are used (inset in Fig. 6).

The correlation between T_{gr} and T_r^{max} has very important consequences. If T_{max} is equal to T_g, the induction time at T_{max} increases with T_{gr} as $1/(1 - T_{gr})^2$; see Eq. (12). For instance, when T_{gr} increases from 0.5 to 0.6, τ increases only by about 1.6 times. However, the decrease observed in T_{max}/T_g with increasing T_{gr} enhances the dependence of $\tau(T_{max})$ on T_{gr} owing to the increase of the exponential term in Eqs. (11) and (12). In the same interval of T_{gr} (0.5–0.6), for instance, the induction

period increases by 2–6 orders of magnitude, depending on the values of C_1 and C_2 and the approximation of viscosity, see Fig. 7. This increased induction time combined with decreased nucleation rate hinder the observation of volume nucleation in glasses having high T_{gr}.

It should be noted that the *slope* of the experimental $\log(\tau(T_r^{max}))$ vs. T_{gr} plot (points in Fig. 7) is quite close to that of the lines calculated in the framework of the CNT with different approximations of viscosity and reasonable C_1 parameters. In contrast, the experimental values of $\log(\tau(T_r^{max}))$ exceed the calculated values by 2–7 orders of magnitude. This discrepancy is likely caused by the approximation $\Delta G_D = \Delta G_\eta$.

Calculations of $I(T)$ similar to those presented here were performed by Turnbull in the 60s [29]. At that time, however, nucleation rate data in wide temperature ranges, including T_{max}, did not exist. It is evident, from Fig. 1, that an abundance of experimental points is required to demonstrate the correlation between I_{max} and T_{gr}. The predicted (by the CNT) and experimentally demonstrated correlation between I_{max} and T_{gr} is consistent with recent theoretical evidence for the increase of the Hruby parameter (which characterizes glass stability on heating) with T_{gr} [30]. In addition, to corroborate our findings, a plethora of experimental data for metallic alloys demonstrates a decrease in critical cooling rate [31] with T_{gr}. In other words, higher T_{gr} leads to lower I_{max} and thus, to more stable glasses.

A few additional comments are given below on reduced glass transition temperatures. According to the Kauzmann rule for glass-forming liquids, the most frequent T_g/T_m or T_g/T_l is 2/3 [24,32]; however, this ratio is widely distributed. Fig. 8(a) shows that only about 10% of the glass-forming substances vitrified at normal cooling rates have $T_{gr} < 0.6$ and, hence, only these 10% show detectable volume nucleation on a laboratory time scale.

In the case of glass-forming metallic alloys, Fig. 8(b), however, most compositions are located at $T_g/T_l < 0.6$, thus nucleating copiously. This fact explains why metallic alloys are reluctant glass-formers compared to the typical glass-formers. The high nucleation rates of metallic glasses make it extremely difficult to measure them. Such data
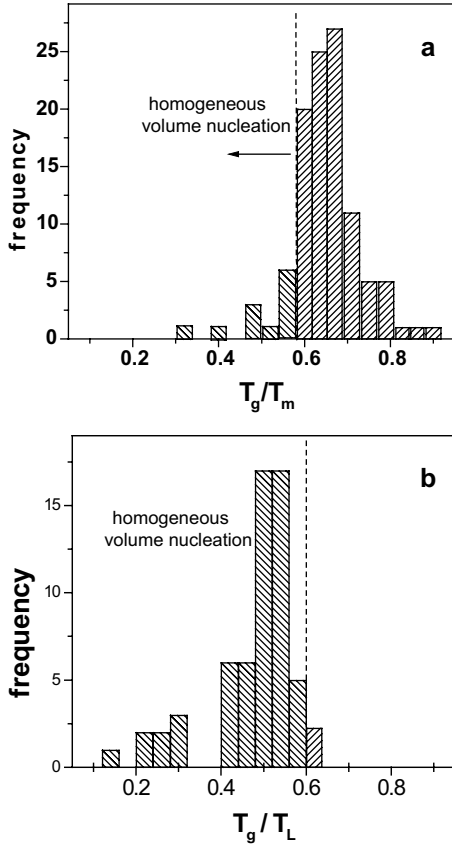
Fig. 8. (a) Frequency distribution histogram of experimentally observed T_g/T_m for 108 typical inorganic glass-formers. (b) Frequency distribution histogram of 80 experimental T_g/T_l for metallic glass-forming alloys [24].

are desirable for an expanded test of the I_{max} vs. T_{gr} dependence, as discussed herein.

6. Conclusions

We verified a significant drop in the nucleation rate maximum, I_{max}, with an increase of reduced glass transition temperature for 51 glass-forming liquids.

An analysis of this remarkable trend reveals that the drastic drop of I_{max} with increased T_{gr} is accompanied by an increase of the temperature of the highest nucleation rate, T_{max}. T_{max} is larger than T_g for low values of T_{gr}, progressively approaches

T_g and then becomes smaller than T_g for increasingly higher T_{gr}. This behaviour greatly increases the induction times, τ, for nucleation at T_{max}. These combined factors (lower I_{max} and higher τ) strongly hinder the experimental observation of homogeneous nucleation in glasses having high glass transition temperatures $T_{gr} > 0.58$.

The correlation between the maximum nucleation rate temperature, induction time and reduced glass transition temperature is confirmed by a plethora of experimental data. All the above-listed trends are qualitatively confirmed by analytical results, within the framework of the CNT.

Appendix A

A.1. The steady-state nucleation rate

The steady-state nucleation rate, I, and time-lag, τ, are given by the following expressions:

$$I \propto \exp\left\{ -C_2'\left(\frac{T_{gr} - T_{or}}{T_r - T_{or}}\right) - \frac{C_1}{T_r(1 - T_r)^2} \right\},$$

(A.1)

$$\tau \propto \frac{1}{(1 - T_r)^2} \exp\left\{ C_2'\left(\frac{T_{gr} - T_{or}}{T_r - T_{or}}\right) \right\}.$$

(A.2)

Here we assume that the activation energy for viscous flow, $\Delta G_\eta = kTC_2'((T_{gr} - T_{or})/(T_r - T_{or}))$, is close to the activation energy, ΔG_D, for diffusional transport of the structural units across the melt/nucleus interface. $C_2'(T_{gr} - T_{or})$ and C_1 characterize the temperature independent parts of the activation energy for viscous flow and of the thermodynamic barrier for nucleation, respectively.

The reduced temperature T_r^{max}, corresponding to the maximum nucleation rate for any given substance (or fixed values of parameters), is then determined via

$$\frac{dI}{dT_r} = I\left\{ C_2'\frac{T_{gr} - T_{or}}{(T_r - T_{or})^2} - C_1\frac{3T_r - 1}{T_r^2(1 - T_r)^3} \right\} = 0$$

(A.3)

or via

$$C_2'(T_{gr} - T_{or}) = C_1 \frac{(3T_r - 1)(T_r - T_{or})^2}{T_r^2(1 - T_r)^3}, \qquad (A.4)$$

$$T_r = T_r^{max}.$$

These results are valid independently of the way one varies the activation energy for viscous flow, ΔG_η, and, correspondingly, the glass transition temperature. In general, however, the results may deviate whether we vary either $C_2(C_2')$ or T_{or}. This way, we will analyze the two possible limiting cases separately.

A.1.1. First method

The reduced Kauzmann temperature T_{or} is assumed to be equal for all glasses.

In this case, we vary T_{gr} by changing the independent parameter $C_2 = C_2'(T_{gr} - T_{or})$. Consequently, the steady-state nucleation rate maximum, $I_{max}(T_r = T_r^{max})$ becomes a function of T_{gr}. We then have

$$I \propto \exp\left\{ -C_2'\left(\frac{T_{gr} - T_{or}}{T_r^{max} - T_{or}}\right) - \frac{C_1}{T_r^{max}(1 - T_r^{max})^2} \right\},$$

$$T_r^{max} = T_r^{max}(T_{gr}), \qquad (A.5)$$

resulting in

$$\frac{dI_{max}}{dT_{gr}} = \frac{\partial I_{max}}{\partial T_{gr}} + \frac{\partial I_{max}}{\partial T_r^{max}} \frac{dT_r^{max}}{dT_{gr}} = \frac{\partial I_{max}}{\partial T_{gr}}. \qquad (A.6)$$

Here we took Eq. (A.3) into account.

After performing the required calculations, we arrive at

$$\frac{d \ln I_{max}}{dT_{gr}} = -\frac{C_2'}{(T_r^{max} - T_{or})}. \qquad (A.7)$$

For any given value of T_{gr}, T_r^{max} is given by Eq. (A.4).

By taking the derivative of Eq. (A.4), we get

$$\frac{dT_r^{max}}{dT_{gr}} = \frac{C_2'}{C_1} \left[\frac{\partial}{\partial T_r}\left(\frac{(3T_r - 1)(T_r - T_{or})^2}{T_r^2(1 - T_r)^3} \right)_{T_r = T_r^{max}} \right]^{-1} \qquad (A.8)$$

with

$$\frac{\partial}{\partial T_r}\left(\frac{(3T_r - 1)(T_r - T_{or})^2}{T_r^2(1 - T_r)^3} \right)$$

$$= \frac{(T_r - T_{or})}{T_r^3(1 - T_r)^4}[(T_r - T_{or})(12T_r^2 - 8T_r + 2)$$

$$+ 2T_r(1 - T_r)(3T_r - 1)]. \qquad (A.9)$$

This way, for reasonable values of the parameters $(T_{or} > 1/3, T_r > T_{or})$, T_r^{max} always increases with increasing values of T_{gr}.

However, the ratio T_r^{max}/T_{gr} behaves differently. For this quantity we may write

$$\frac{d}{dT_{gr}}\left(\frac{T_r^{max}}{T_{gr}} \right) = \frac{1}{T_{gr}} \frac{dT_r^{max}}{dT_{gr}} - \frac{T_r^{max}}{T_{gr}^2}$$

$$= \frac{T_r^{max}}{T_{gr}^2}\left[\frac{T_{gr}}{T_r^{max}} \frac{dT_r^{max}}{dT_{gr}} - 1 \right]. \qquad (A.10)$$

With Eqs. (A.4), (A.8), and (A.9), we have then

$$\frac{T_{gr}}{T_r^{max}} \frac{dT_r^{max}}{dT_{gr}} = \frac{1}{2}\left(\frac{T_{gr}}{T_r^{max}} \right)$$

$$\times \frac{(T_r^{max} - T_{or})}{1 + (T_r^{max} - T_{or})\frac{6(T_r^{max})^2 - 4T_r^{max} + 1}{T_r^{max}(1 - T_r^{max})(3T_r^{max} - 1)}}. \qquad (A.11)$$

For realistic parameter values, in general, the relation

$$\frac{T_{gr}}{T_r^{max}} \frac{dT_r^{max}}{dT_{gr}} < 1 \qquad (A.12)$$

is fulfilled and the ratio T_r^{max}/T_{gr} decreases with increasing values of T_{gr}.

A.1.2. Second method

$C_2 = C_2'(T_{gr} - T_{or})$ is considered as a constant.

We assume now that $C_2 = C_2'(T_{gr} - T_{or})$ is a constant. Hence, T_{or} can be varied as an independent parameter resulting immediately in variations of T_{gr}, again. Here, instead of Eqs. (A.4) and (A.5), we have to start then with

$$C_2 = C_1 \frac{(3T_r - 1)(T_r - T_{or})^2}{T_r^2(1 - T_r)^3}, \quad T_r = T_r^{max}, \quad (A.13)$$

$$I \propto \exp\left\{ -\left(\frac{C_2}{T_r^{max} - T_{or}} \right) - \frac{C_1}{T_r^{max}(1 - T_r^{max})^2} \right\}. \qquad (A.14)$$

Initially, we conclude thus from Eq. (A.13) that T_r^{max} can be considered as a function of T_{or} (see also Eq. (A.8)). However, $T_{or} = T_{gr} - C_2/C_2'$ holds. Thus, T_{or} and T_{gr} differ by a constant, only. By this reason, T_r^{max} can be also considered a function of T_{gr}. Instead of Eq. (A.6), we then have

$$\frac{dI_{max}}{dT_{gr}} = \frac{dI_{max}}{dT_{or}}\frac{dT_{or}}{dT_{gr}} = \frac{\partial I_{max}}{\partial T_{or}} + \frac{\partial I_{max}}{\partial T_r^{max}}\frac{dT_r^{max}}{dT_{or}} = \frac{\partial I_{max}}{\partial T_{or}}$$

(A.15)

and, since $dT_{or}/dT_{gr} = 1$ holds, one gets

$$\frac{d\ln I_{max}}{dT_{gr}} = -\frac{C_2}{(T_r^{max} - T_{or})^2}$$
$$= -\frac{C_2}{\left(T_r^{max} - T_{gr} + \dfrac{C_2}{C_2'}\right)^2}.$$

(A.16)

Similarly to the previously investigated case (A.1.1), I^{max} is a decreasing function of T_{gr}.

To estimate the kind of variation of T_r^{max} with T_{gr} one can also perform calculations similar to those as given in Section A.1.1. By dividing Eq. (A.13) by C_1 and taking the derivative with respect to T_{or} (or, equivalently, T_{gr}) we arrive at

$$\frac{dT_r^{max}}{dT_{gr}} = -\frac{\dfrac{\partial}{\partial T_{or}}\left(\dfrac{(3T_r - 1)(T_r - T_{or})^2}{T_r^2(1 - T_r)^3}\right)}{\dfrac{\partial}{\partial T_r}\left(\dfrac{(3T_r - 1)(T_r - T_{or})^2}{T_r^2(1 - T_r)^3}\right)}\Bigg|_{T_r = T_r^{max}}.$$

(A.17)

With Eq. (A.9), we get finally

$$\frac{dT_r^{max}}{dT_{gr}} = \frac{1}{1 + (T_r^{max} - T_{or})\dfrac{6(T_r^{max})^2 - 4T_r^{max} + 1}{T_r^{max}(1 - T_r^{max})(3T_r^{max} - 1)}}.$$

(A.18)

It follows that T_r^{max} again increases with increasing values of T_{gr}.

Taking into account that the ratio T_{gr}/T_r^{max} has values near to one, in general, the relation Eq. (A.12) is fulfilled and the ratio T_r^{max}/T_{gr} decreases with increasing values of T_{gr}.

This way, independent on the way, T_{gr} is changed (variations either of C_2 or T_{or}, respectively), I_{max} decreases, T_r^{max} increases and T_r^{max}/T_{gr} decreases with increasing values of T_{gr}.

A.2. The time-lag

Similarly, we obtain for the dependence of the time-lag τ at the respective steady-state nucleation rate maxima the following dependencies:

A.2.1. First method
As in Section A.1.1 we assume that T_{or} is a constant. Then, we get similarly

$$\frac{d\tau(T_r^{max})}{dT_{gr}} = \frac{\partial \tau}{\partial T_{gr}} + \frac{\partial \tau}{\partial T_r}\frac{dT_r}{dT_{gr}}, \quad T_r = T_r^{max}(T_{gr}).$$

(A.19)

After performing the required calculations, we arrive at

$$\frac{d\ln\tau}{dT_{gr}} = \frac{C_2'}{T_r^{max} - T_{or}} + \left[\frac{2}{1 - T_r^{max}} - C_2'\frac{T_{gr} - T_{or}}{(T_r^{max} - T_{or})^2}\right]\frac{dT_r}{dT_{gr}}\Bigg|_{T_r = T_r^{max}}.$$

(A.20)

$T_r^{max}(T_{gr})$ and dT_r/dT_{gr} at $T_r = T_r^{max}$ in Eq. (A.20) have to be determined via Eq. (A.4).

Since $T_{gr} \approx T_r^{max}$ and $T_r^{max}/T_{gr} \ll 1$ holds (cf. Eq. (A.11)), $\ln \tau$ is an increasing function of T_{gr}.

A.2.2. Second method
We assume, as in Section A.1.2, that $C_2 = C_2'(T_{gr} - T_{or})$ is a constant and that T_{or} or T_{gr} is an independent parameter. Instead of Eq. (A.2), we have to start with

$$\tau \propto \frac{1}{(1 - T_r)^2}\exp\left\{\left(\frac{C_2}{T_r - T_{or}}\right)\right\}.$$

(A.21)

Similarly to Eqs. (A.15) and (A.19), we then get

$$\frac{d\tau(T_r^{max})}{dT_{gr}} = \frac{\partial \tau}{\partial T_{or}} + \frac{\partial \tau}{\partial T_r}\frac{dT_r}{dT_{or}}, \quad T_r = T_r^{max}(T_{or}).$$

(A.22)

$T_r^{max}(T_{or})$ and dT_r/dT_{or} at $T_r = T_r^{max}$ in Eq. (A.22) have to be determined via Eq. (4), again. After some algebra, we have

$$\frac{d\ln\tau}{dT_{gr}} = \frac{C_2'}{T_r^{max} - T_{or}} + \left[\frac{2}{1 - T_r^{max}} - \frac{C_2}{(T_r^{max} - T_{or})^2}\right]\frac{dT_r}{dT_{or}}\Bigg|_{T_r = T_r^{max}}.$$

(A.23)

Since $\mathrm{d}T_{\mathrm{r}}^{\max}/\mathrm{d}T_{\mathrm{or}} = \mathrm{d}T_{\mathrm{r}}^{\max}/\mathrm{d}T_{\mathrm{gr}} < 1$ holds (cf. Eq. (A.18)), $\ln \tau$ is an increasing function of T_{gr}.

Thus, the following changes of the nucleation parameters with *increasing* the reduced glass transition temperature are evident from the performed analysis, independent on the way of changing T_{gr} (variation of C_2 or T_{or}):

- Decrease in $I_{\max}$.
- Increase of $T_{\mathrm{r}}^{\max}$.
- Decrease in the ratio $T_{\mathrm{r}}^{\max}/T_{\mathrm{gr}}$.
- Increase of time-lag at $T_{\max}$.

All these conclusions are consistent with the numerical calculations and experimental data.

References

[1] G. Tammann, Z. Elektrochem. 10 (1904) 532.

[2] P.F. James, Volume nucleation in silicate glasses, in: M.H. Lewis, (Ed.), Glasses and Glass–Ceramics, 1989.

[3] E.D. Zanotto, J. Non-Cryst. Solids 89 (1987) 361.

[4] E.D. Zanotto, M.C. Weinberg, Phys. Chem. Glasses 30 (1989) 186.

[5] J. Deubener, Glastech. Ber. Glass Sci. Technol. C 1 (73) (2000) 178.

[6] J. Deubener, J. Non-Cryst. Solids 274 (2000) 195.

[7] J. Deubener, Proc. XIX Int. Congr. Glass., vol. 2, Extended Abstracts, Ed. Soc. Glass Tech., Edinburgh, 2001, p. 66.

[8] V.M. Fokin, N.S. Yuritsin, Glass Phys. Chem. 23 (1997) 236.

[9] V.N. Filipovich, A.M. Kalinina, G.A. Sycheva, Inorg. Mater. 11 (1975) 1305.

[10] L.L. Burgner, M.C. Weinberg, J. Non-Cryst. Solids 261 (2000) 163.

[11] T. Wakasugi, L.L. Burgner, M.C. Weinberg, J. Non-Cryst. Solids 244 (1999) 63.

[12] O.V. Potapov, V.M. Fokin, V.L. Ugolkov, L.Y. Suslova, V.N. Filipovich, Glass Phys. Chem. 26 (2000) 39.

[13] O.V. Potapov, V.M. Fokin, V.N. Filipovich, J. Non-Cryst. Solids 247 (1999) 74.

[14] V.M. Fokin, A.M. Kalinina, V.N. Filipovich, J. Cryst. Growth 52 (1980) 115.

[15] A.M. Kalinina, V.N. Filipovich, V.M. Fokin, G.A. Sycheva, in: Proc. Int. Cong. on Glass, New Dehli, vol. 1, 1986, p. 366.

[16] A.M. Kalinina, V.M. Fokin, V.N. Filipovich, J. Non-Cryst. Solids 38&39 (1980) 723.

[17] L. Granasy, T. Wang, P.F. James, J. Chem. Phys. 108 (1998) 7317.

[18] K. Lakshmi Narayan, K.F. Kelton, J. Non-Cryst. Solids 220 (1997) 222.

[19] C.J.R. Gonzalez-Oliver, PhD thesis, Sheffield University, 1979.

[20] P.F. James, in: J.H. Simmons, D.R. Uhlmann, G.H. Beall (Eds.), Advances in Ceramics, American Ceramic Society, Columbus, OH, 1982, p. 1.

[21] V.M. Fokin, A.M. Kalinina, V.N. Filipovich, Glass (Proc. of Institute of Glass) 148 (1975) 74.

[22] Z. Strnad, R.W. Douglas, Phys. Chem. Glasses 14 (1973) 33.

[23] A. Bondarenko, bachelor thesis, St. Petersburg, 2001.

[24] I. Gutzow, J. Schmelzer, The Vitreous State: Thermodynamics, Structure, Rheology and Crystallization, Springer, Berlin, 1995, p. 469.

[25] K.F. Kelton, Solid State Phys. 45 (1991) 75.

[26] S. Manrich, E.D. Zanotto, Cerâmica 41 (271) (1995) 105 (in Portuguese).

[27] V.N. Filipovich, A.M. Kalinina, V.M. Fokin, in: E.A. Porai-Koshits (Ed.), Stekloobraznoe sostoyanie, Leningrad, 1983, p. 124 (in Russian).

[28] M.H. Lewis, J. Metacalf-Johansen, P.S. Bell, J. Am. Ceram. Soc. 62 (5–6) (1979) 278.

[29] D. Turnbull, in: J.A. Prins (Ed.), Physics of Non-Crystalline Solids, North-Holland, Amsterdam, 1964, p. 41.

[30] I. Avramov, E.D. Zanotto, M.O. Prado, J. Non-Cryst. Solids, 320 (2003) 9.

[31] M.O. Prado, private communication, 2002.

[32] S. Sakka, J.D. Mackenzie, J. Non-Cryst. Solids 6 (1971) 145.